Biodistribution and Dosimetry of ^{99m}Tc-RP527, a Gastrin-Releasing Peptide (GRP) Agonist for the Visualization of GRP Receptor–Expressing Malignancies

Christophe Van de Wiele, Filip Dumont, Rudi A. Dierckx, Susan H. Peers, John R. Thornback, Guido Slegers, and Hubert Thierens

Division of Nuclear Medicine, University Hospital Ghent, Ghent; Department of Radiopharmacy and Department of Biomedical Physics and Radiation Protection, University Ghent, Ghent, Belgium; and Resolution Pharmaceuticals Inc., Mississauga, Ontario, Canada

The aim of this study was to determine the human biodistribution and radiation dosimetry of ^{99m}Tc-RP527, a promising radioligand for the visualization of gastrin-releasing peptide (GRP) receptor–expressing human malignancies. **Methods:** Whole-body scans were obtained up to 48 h after intravenous injection of 555 MBq ^{99m}Tc-RP527 in each of 6 subjects. Blood samples were taken at various times up to 48 h after injection. Urine was collected up to 48 h after injection for calculation of renal clearance and whole-body clearance. Time–activity curves were generated for the thyroid, heart, breasts in women, testes in men, and liver by fitting the organ-specific geometric mean counts, obtained from regions of interest, on the respective images as a function of the time after injection. The MIRD formulation was applied to calculate the absorbed radiation dose for various organs. **Results:** The serial whole-body images showed rapid hepatobiliary excretion, resulting in low background and potentially high-contrast imaging of the thoracic region. Imaging of abdominal tumors may prove problematic, however, because of the extensive bowel activity. ^{99m}Tc-RP527 was predominantly cleared by the kidneys and to a lesser extent by the gastrointestinal tract. The mean excretion in the urine ($\pm$SD) at 48 h after injection was 58.3 $\pm$ 5.4 percentage of the injected activity corrected for decay to the time of injection. The highest absorbed doses were received by the excretory organs (i.e., the urinary bladder and gallbladder wall). The average effective dose of ^{99m}Tc-RP527 was estimated to be 0.0095 mSv/MBq. **Conclusion:** The biodistribution of ^{99m}Tc-RP527 revealed low lung, myocardial, and liver uptake, which allowed early imaging of the supradiaphragmatic region with a favorable dosimetry (including effective dose) for administered activities required for SPECT imaging.

Key Words: ^{99m}Tc-RP527; biodistribution; dosimetry

J Nucl Med 2001; 42:1722–1727

Gastrin-releasing peptide (GRP) belongs to the family of bombesin-like peptides (BLPs) that includes the amphibian peptide bombesin as well as the mammalian counterpart GRP and neuromedin B (*1*). Aside from their physiologic role (e.g., stimulation of secretion of gastrin and pancreatic enzymes and gallbladder contraction) (*2,3*), BLPs have been shown to play a role in various tumor models and human cancer (*4–13*).

In humans, both GRP and GRP antagonists mediate their action through the membrane-bound G-protein–coupled GRP receptor (GRP-R) (*14*). GRP receptors have been detected in various types of human carcinoma (*15–17*). The presence or absence of receptors on tumor cells, including GRP-R, as well as their level of expression have been correlated with cancer prognosis in several settings (*18–22*).

In analogy to the diagnosis of somatostatin receptor–expressing tumors in vivo with somatostatin receptor scintigraphy, in vivo GRP-R scintigraphy may be a potentially valuable tool to visualize and semiquantitate tumor GRP expression in a noninvasive way. This may allow prediction of therapy responsiveness to GRP antagonists and in vivo prognosis stratification. ^{99m}Tc-RP527 is a targeting peptide derived from bombesin linked at its N-terminus through a linker group to a peptide sequence that chelates ^{99m}Tc. ^{99m}Tc-RP527 binds GRP-Rs with similar affinity to bombesin and is taken up by prostate, pancreas, and breast tumor tissue in animal models as well as in humans in vivo (*23,24*). This article reports on its biodistribution and dosimetry in humans.

MATERIALS AND METHODS

Radiopharmaceutical Synthesis

^{99m}Tc-RP527 labeling was performed using a kit formulation; the reaction mixture contains 0.1 mL stannous chloride (2 mmol/L), 0.1 mL sodium gluconate (60 mmol/L), 1,850–2,035 MBq ^{99m}TcO$_4$ in 0.3 mL sodium chloride (0.9%), 0.5 mL sodium chlo-

ride (0.9%), and 100 μg RP527. After 35 min in a boiling water bath, the reaction mixture was allowed to cool to room temperature and injected on a high-performance liquid chromatography system using a gradient of ethanol, water, and acetic acid. The radiolabeled peptide was collected at 45 min, and the collected eluent was diluted with 10 mL sodium chloride (0.9%). The overall yield of the radiosynthesis was approximately 30% with a radiochemical purity of ≥90% and a specific activity of ≥4.32 TBq/Gmmol.

Subjects

This study was approved by the Medical Ethics Committee of the University Hospital Ghent and performed according to good clinical practice. Six individuals (3 men, 3 women; mean age, 46 y; age range, 24–73 y) were included in the study. All subjects gave their written informed consent for participation in the study. All volunteers were free from illness on the basis of screening by medical history, physical examination, serum chemical analyses, complete blood cell count, and urinalysis. Because of safety concerns, all chemical analyses were repeated during the experiment and the results were compared to their baseline (screening) values.

Imaging

Subjects were positioned supine with their arms alongside their body. Whole-body images were obtained using a triple-head gamma camera (Irix; Picker International, Cleveland Heights, OH) equipped with low-energy, high-resolution, parallel-hole collimators. The energy peak was centered at 140 keV with a 15% window. Whole-body planar images were acquired at approximately 30 min and 1, 3, 6, 24, and 48 h after injection. Acquisition was performed simultaneously in anterior and posterior positions with a scan speed of 11.4 cm/min. The matrix size was 256 × 1,024 pixels.

Urine Sampling

For all subjects, all voided urine from the time of injection until 48 h after injection was collected. The subjects were requested to collect urine before each emission scan and at home ad libitum. For each voiding, the urine was collected in a separate container, and the volume and time of voiding were recorded. For each void time, two 1-mL urine aliquots were sampled, and radioactivity was counted in a NaI(Tl) counter (Cobra; Packard Instrument Co., Downers Grove, IL) after the counting efficiency of the system had been determined. The amount of radioactivity in the urine at each void time was expressed as percentage of the injected activity corrected for decay to the time of injection (%IA) of ⁹⁹ᵐTc-RP527.

Blood Sampling

Blood samples were taken at 15 s, 30 s, 45 s, 1 min, 1 min 15 s, 1 min 30 s, 2 min, 5 min, 7 min 30 s, 10 min, 12 min, 15 min, 20 min, 30 min, 55 min, 2 h, 4 h, 6 h, 24 h, and 48 h after injection of the tracer. Duplicate 1-mL aliquots from each blood sample were assayed for ⁹⁹ᵐTc radioactivity as described above. Total blood volume and, consequently, activity were calculated using a total blood volume based on body weight and height (25) and expressed as %IA.

Dosimetry

Image Analysis. For quantification of radioactivity uptake after injection of ⁹⁹ᵐTc-RP527, regions of interest (ROIs) over the total body and organs of interest were drawn manually on the earliest images, and the shapes and sizes (i.e., number of pixels) were kept constant over all subsequent images. Correction for background

counts was performed using a region over the shoulder and subtracting the mean counts per pixel in the background ROI from the mean counts per pixel in each organ's ROI to yield net counts in each organ. For each ROI (i.e., each organ), the geometric mean, corrected for physical decay, of total anterior and posterior counts was calculated. The total-body geometric mean activity calculated on the first image (1 h after injection) was taken as the total injected activity, considering that no urine was excreted before the first whole-body scan. The activity in the total body and different organs was expressed as %IA calculated by the following equation: (geometric mean net counts in organ or total body)/(geometric mean counts in first total body) × 100.

Dosimetric Calculations. For each individual, time–activity curves were generated for the thyroid, heart, breasts in women, testes in men, liver, and whole body. Using in-house curve-fitting software, time–activity curves were generated for these organs by biexponential fits. Two routes of excretion were considered: urinary and fecal excretion. The fecal excretion was predicted using data from the source organs, the urinary excretion, and the material excreted by the liver. Of the material excreted by the liver, 30% was assumed to flow directly in the small intestine. Activity in the small intestine was assumed to follow the gastrointestinal kinetic model in International Commission on Radiobiological Protection Publication 30 (26). Activity in the intestines was assumed to pass through the various segments at standard rates, with mean transit times of 4 h for the small intestine, 13 h for the upper large intestine, and 24 h for the lower large intestine. The transfer rate coefficient from the gallbladder to the small intestine was taken to be 1.8 h⁻¹, derived by taking the mean of average emptying rates reported by others (27).

Source organ residence times were determined from analytic integration of the time–activity curves. Residence times were then used to determine target organ radiation doses based on the MIRD methodology (28) for the normal adult (29) using the MIRDOSE software package (30).

RESULTS

After injection of approximately 555 MBq ⁹⁹ᵐTc-RP527 (maximum, 3 ng/kg per subject), no short-term adverse or subjective effects were noted in any of the subjects. Their vital signs remained stable throughout the experiment. Moreover, no meaningful changes were observed in any of the clinical laboratory assays performed on the blood and urine specimens obtained at 1, 6, 24, and 48 h after administration of the radioligand when compared with baseline findings. Figure 1 presents whole-body images of a male and female subject showing the biodistribution of radioactivity on injection of ⁹⁹ᵐTc-RP527 at different time points after injection. The whole-body images obtained between 30 min and 24 h after injection show most of the activity distributed in the bladder, liver, gallbladder, and intestines, reflecting the known urinary and hepatobiliary excretion of peptides. Although the kidneys were not visualized in all subjects, there was activity in the urinary bladder in all subjects, indicating prompt excretion through the renal system. Uptake in the brain, myocardium, and lungs was low. There was a diffuse uptake and retention of radioactivity in the normal breast tissue in women as well as in the testes in
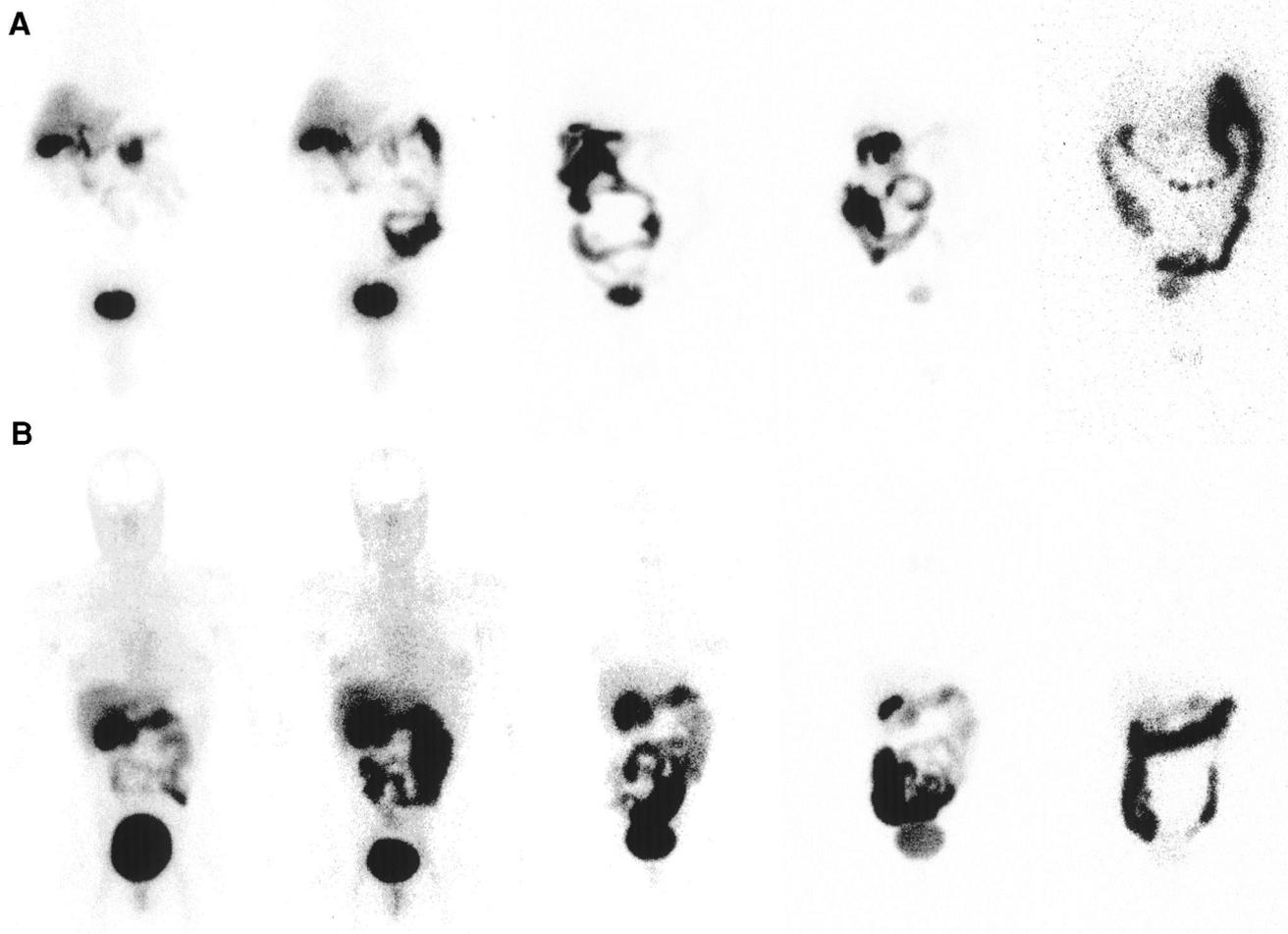
FIGURE 1. Anterior whole-body images obtained from man (A) and woman (B) at 30 min and 1, 3, 6, and 24 h after injection.

men. Although images at 24 and 48 h after injection were of low quality (attributed to low counting statistics), these images showed most of the remaining activity distributed in the intestines. Figure 2 presents averaged ROI data, over all subjects (expressed as %IA), of the biodistribution of ^{99m}Tc-RP527 in the total body and in various organs at the different points in time. Clearance of radioactivity from blood and organs fitted a biexponential curve. Assays of blood samples showed that the elimination of activity from the blood was initially fast: by 20 min after injection, <20% of the injected dose remained in the blood. The mean calculated half-life was 1.5 min (first exponent).

The average excretion fractions of the 6 subjects predicted for feces and measured for urine are given in Table 1. Most of the administered activity was eliminated by the renal system. The mean cumulative total measured urinary excretion ($\pm$SD) of the 6 subjects at 48 h after injection was 58.3 ± 5.4 %IA, whereas the mean predicted %IA excreted in the feces ($\pm$SD) was 3.9 ± 0.8 %IA at 48 h after injection.

The residence time was highest for the remainder of the body in all subjects. This value was followed by the urinary bladder and the liver (Table 2).

The mean radiation dose estimates ($\pm$SD) were calculated for each subject independently and then averaged (Table 3). The organs receiving the highest absorbed doses were involved in the excretion of ^{99m}Tc-RP527 from the body. On average, the highest dose was received by the urinary bladder ($9.63 \times 10^{-2} \pm 1.16 \times 10^{-2}$ mGy/MBq) followed by the gallbladder wall ($1.69 \times 10^{-2} \pm 4.32 \times 10^{-3}$ mGy/MBq) and the testes ($1.23 \times 10^{-2} \pm 2.70 \times 10^{-3}$ mGy/MBq). The estimated mean effective dose ($\pm$) for the adult subject was $9.53 \times 10^{-3} \pm 1.06 \times 10^{-3}$ mSv/MBq.

DISCUSSION

This study shows the biodistribution and kinetics of ^{99m}Tc-RP527 in humans. Its dosimetry is comparable with that of other ^{99m}Tc-labeled diagnostic radiopharmaceuticals. Moreover, although limited in terms of safety, the results of this study indicate that ^{99m}Tc-RP527 is a pharmacologically safe radioligand because it did not produce any demonstrable pharmacologic effects in the short term. The lack of a pharmacologic effect was expected because the dose injected (± 3 ng/kg) was only half of the dose of unlabeled bombesin reported to induce side effects (e.g., nausea, vomiting) (*31*).
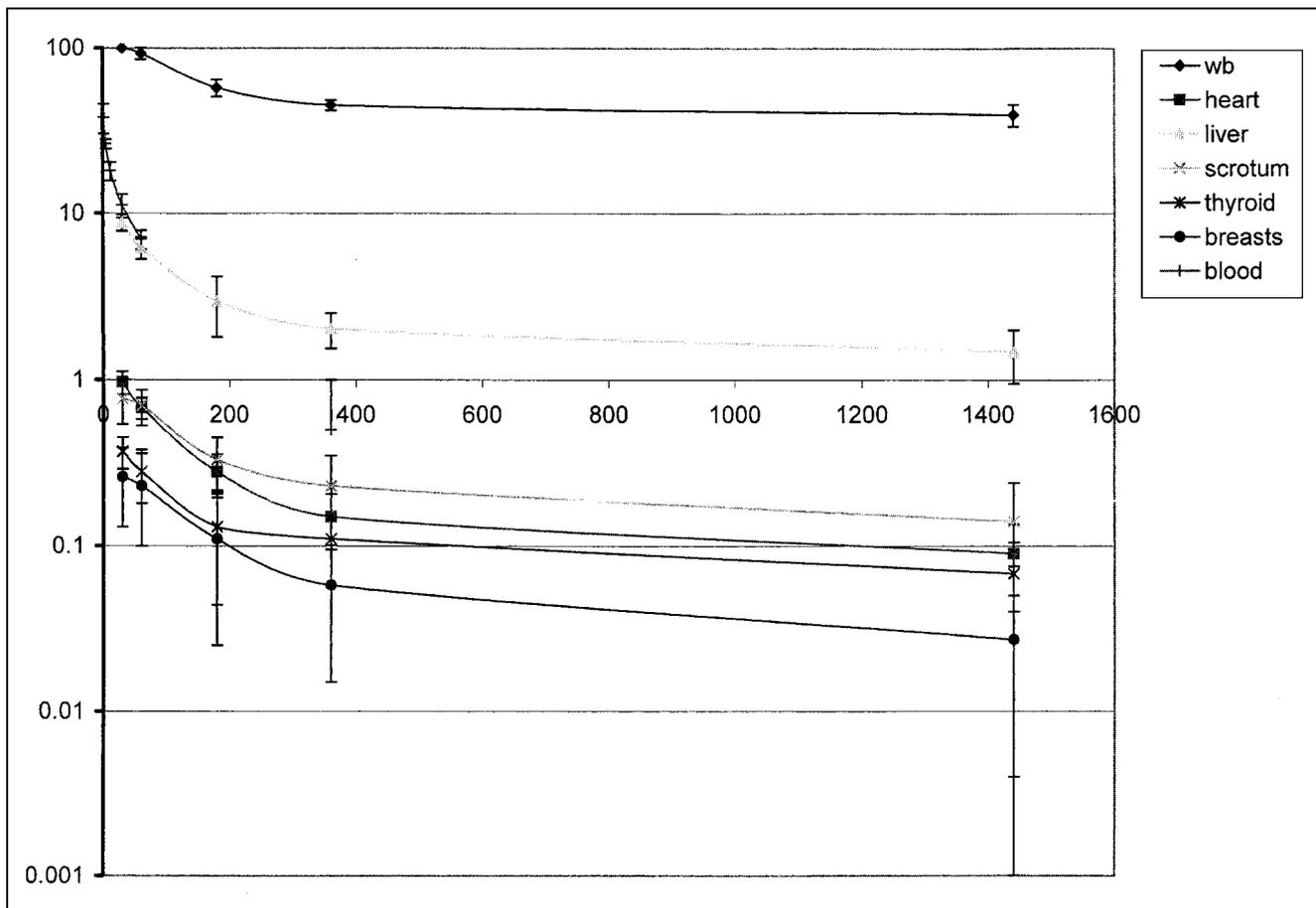
FIGURE 2. Time–activity curves for total body (wb), various organs, and blood, calculated from direct measurements of counts in organ-specific ROIs or in blood. Physical decay-corrected data (expressed as %IA) are averaged over 6 subjects, except for breasts ($n = 3$) and testes ($n = 3$). Error bars represent 1 SD. Units of abscissa and ordinate are time (h) and %IA, respectively. Respective biexponential functions obtained for various ROIs and whole body are whole body, $y = 38.16e^{-0.00001 \times t} + 65.90e^{-0.00569 \times t}$ ($r = 0.96528$); heart, $y = 0.18e^{-0.0005 \times t} + 1.19e^{-0.0140 \times t}$ ($r = 0.99898$); liver, $y = 2.36e^{-0.0003 \times t} + 10.17e^{-0.0154 \times t}$ ($r = 0.99893$); scrotum, $y = 0.19e^{-0.0002 \times t} + 0.77e^{-0.0083 \times t}$ ($r = 0.99015$); thyroid, $y = 0.12e^{-0.0004 \times t} + 0.41e^{-0.0156 \times t}$ ($r = 0.99881$); breasts, $y = 0.03e^{-0.0002 \times t} + 0.28e^{-0.0069 \times t}$ ($r = 0.99705$); and blood, $y = 23.57e^{-0.1842 \times t} + 18.44e^{-0.0163 \times t}$ ($r = 0.99963$).

In humans, ^{99m}Tc-RP527 was cleared rapidly from circulation: by 20 min after injection, <20% of the injected dose remained in the blood. The mean calculated blood clearance half-life of 1.5 min for ^{99m}Tc-RP527 is comparable with the 2.2 min for unlabeled bombesin reported in men (32). Low brain, lung, and myocardial uptake and rapid hepatobiliary excretion of ^{99m}Tc-RP527 resulted in excellent imaging conditions for the supradiaphragmatic region, even at early time points (1 h) after injection. On the other hand, in addition to a predominant urinary clearance, ^{99m}Tc-RP527 was also cleared enterohepatically, resulting in a high ac-

TABLE 1
Excretion Fractions (%IA) for ^{99m}Tc-RP527

Compartment	Time after injection (h)	Average ± SD
Urine	48, measured	58.3 ± 5.4
Feces	48, predicted	3.9 ± 0.8

TABLE 2
Residence Times (h) for ^{99m}Tc-RP527 for Each Source Organ

Organ	Average ± SD
Gallbladder	0.106 ± 0.031
Lower large intestine	0.031 ± 0.009
Small intestine	0.048 ± 0.015
Upper large intestine	0.063 ± 0.019
Heart wall	0.025 ± 0.004
Liver	0.264 ± 0.053
Thyroid	0.012 ± 0.007
Bladder	1.801 ± 0.206
Remainder	2.325 ± 0.197
Breasts*	0.009 ± 0.007
Testes†	0.028 ± 0.007

*$n = 3$ women.
†$n = 3$ men.

TABLE 3
Radiation Absorbed Dose Estimates (mGy/MBq) for ^{99m}Tc-RP527

Target organ	Average ± SD
Adrenals	$2.27 \times 10^{-3} \pm 3.55 \times 10^{-4}$
Brain	$1.23 \times 10^{-3} \pm 1.84 \times 10^{-4}$
Gallbladder wall	$1.69 \times 10^{-2} \pm 4.32 \times 10^{-3}$
Lower large intestinal wall	$7.27 \times 10^{-3} \pm 8.68 \times 10^{-4}$
Small intestine	$4.53 \times 10^{-3} \pm 5.98 \times 10^{-4}$
Stomach	$2.12 \times 10^{-3} \pm 3.20 \times 10^{-4}$
Upper large intestinal wall	$5.46 \times 10^{-3} \pm 9.65 \times 10^{-4}$
Heart wall	$2.64 \times 10^{-3} \pm 5.75 \times 10^{-4}$
Kidneys	$2.17 \times 10^{-3} \pm 3.04 \times 10^{-4}$
Liver	$4.79 \times 10^{-3} \pm 1.13 \times 10^{-3}$
Lungs	$1.71 \times 10^{-3} \pm 3.23 \times 10^{-4}$
Muscle	$2.40 \times 10^{-3} \pm 2.73 \times 10^{-4}$
Pancreas	$2.57 \times 10^{-3} \pm 3.86 \times 10^{-4}$
Red marrow	$2.18 \times 10^{-3} \pm 2.68 \times 10^{-4}$
Bone surfaces	$3.46 \times 10^{-3} \pm 4.07 \times 10^{-4}$
Skin	$1.25 \times 10^{-3} \pm 1.47 \times 10^{-4}$
Spleen	$1.80 \times 10^{-3} \pm 2.74 \times 10^{-4}$
Thymus	$1.56 \times 10^{-3} \pm 2.49 \times 10^{-4}$
Thyroid	$8.07 \times 10^{-3} \pm 3.90 \times 10^{-3}$
Urinary bladder wall	$9.63 \times 10^{-2} \pm 1.16 \times 10^{-2}$
Uterus*	$1.08 \times 10^{-2} \pm 1.15 \times 10^{-3}$
Testes†	$1.23 \times 10^{-2} \pm 2.70 \times 10^{-3}$
Ovaries*	$6.75 \times 10^{-3} \pm 5.17 \times 10^{-4}$
Breasts*	$9.59 \times 10^{-4} \pm 2.28 \times 10^{-4}$
Total body	$2.54 \times 10^{-3} \pm 3.17 \times 10^{-4}$
Effective dose equivalent‡	$1.13 \times 10^{-2} \pm 1.12 \times 10^{-3}$
Effective dose‡	$9.53 \times 10^{-3} \pm 1.06 \times 10^{-3}$

*$n = 3$ women.

†$n = 3$ men.

‡Units of effective dose equivalent and effective dose are mSv/MBq.

cumulation of radioactivity affecting interpretation of the abdominal region.

Of interest is the visualization of the breasts in women and the testes in men. Visualization of the breasts is in keeping with the known bombesin-like immunoreactivity shown in mammary glands of various species (33,34), indicating that bombesin or GRP may be involved in the regulation of mammary cell proliferation and differentiation. Data by Halmos et al. (35) showing a highly positive correlation ($r = 0.671$; $P < 0.005$) between the binding capacity of high-affinity (Tyr4)-bombesin binding sites and estrogen receptor levels and between the concentration of low-affinity (Tyr4)-bombesin binding sites and peptide receptor levels ($r = 0.541$; $P < 0.005$) in biopsies of human breast carcinoma suggest a possible interaction with other receptor systems.

In primates, a bombesin-like peptide resulting from alternate splicing of the GRP gene has been detected in testis. In vitro, GRP at a concentration of 100 nmol/L, added after ionophore treatment, enhanced significantly ($P < 0.05$) human sperm motility, capacitation, zona binding, and ac-

rosome reaction, thus supporting a role for BLPs in the regulation of sperm cell proliferation and differentiation (36). In this regard, the visualization of the testes in all 3 male subjects after injection of ^{99m}Tc-RP527 suggests the presence of a currently unidentified human testicular BLP receptor. Because NMB-R gene expression is prominent in mouse testis and the BRS-3 receptor has been shown to be expressed in rat testis, it is possible that different subtypes of bombesin receptors mediate the same response in different species (37).

The MIRDOSE software provides a calculation of the effective dose as defined in International Commission on Radiological Protection (ICRP) Publication 60 (38). On the basis of the mean effective dose of 9.5×10^{-3} mSv/MBq obtained in this study, patients and volunteers could easily be investigated with 555 MBq ^{99m}Tc-RP527, allowing both planar and SPECT imaging. The corresponding effective dose of 5.27 mSv is equal to the reported average effective dose per patient from nuclear medicine procedures in Europe (39) and only half of the 10-mSv upper-limit average effective dose of category IIa of the World Health Organization and category IIb of the ICRP (40). Because the highest dose is received by the bladder wall, frequent voiding will reduce the absorbed dose to the urinary bladder. Given the 1% probability for severe hereditary disorders in the offspring per Sv received by the testis, the associated risk related to injection of 555 MBq ^{99m}Tc-RP527 is <1 per 10,000. This risk is low compared with the 1.6% prevalence of naturally occurring genetic disorders (38).

CONCLUSION

The biodistribution of ^{99m}Tc-RP527 showed low lung, myocardial, and liver uptake, which allowed early imaging of the supradiaphragmatic region with a dosimetry favorable for clinical SPECT imaging.

ACKNOWLEDGMENTS

REFERENCES

1. Erspamer V. Discovery, isolation and characterization of bombesin-like peptides. *Ann N Y Acad Sci.* 1998;547:3–9.
2. Delle Fave G, Annibale B, De Magistris L, et al. Bombesin effects on human GI functions. *Peptides.* 1985;6:113–116.
3. Bruzzone R, Tamburanno G, Lala A, et al. Effect of bombesin on plasma insulin, pancreatic glucagon and gut glucagon in man. *J Clin Endocrinol Metab.* 1983;56:643–647.
4. Rozengurt E. Bombesin stimulation of mitogenesis: specific receptors, signal transduction and early events. *Am Rev Respir Dis.* 1990;142(suppl):S11–S15.
5. Cuttita F, Carney DN, Mulshine J, et al. Bombesin-like peptides can function as autocrine growth factors in human small-cell lung cancer. *Nature.* 1985;316:825–828.
6. Carney DN, Cuttita F, Moody TW, Minna JD. Selective stimulation of small cell lung cancer clonal growth by bombesin and gastrin-releasing peptide. *Cancer Res.* 1987;47:821–825.
7. Moody TW, Cuttita F. Growth factor and peptide receptors in small cell lung cancer. *Life Sci.* 1993;52:1161–1173.
8. Bologna M, Festuccia C, Muzi P, Biordi L, Ciomei M. Bombesin stimulates growth of human prostatic cancer cells in vitro. *Cancer.* 1989;63:1714–1720.

9. Nelson J, Donnelly M, Walker B, Gray J, Shaw C, Murphy RF. Bombesin stimulates proliferation of human breast cancer cells in culture. *Br J Cancer.* 1991;63:933–936.

10. Yano TY, Pinski J, Groot K, Schally AV. Stimulation of bombesin and inhibition by bombesin gastrin-releasing peptide antagonist RC-3095 of growth of human breast cancer cell lines. *Cancer Res.* 1992;52:4545–4547.

11. Pinski J, Reile H, Halmos G, Groot K, Schally AV. Inhibitory effects of somatostatin analogue RC-160 and bombesin/gastrin-releasing peptide antagonist RC-3095 on the growth of the androgen-independent Dunning R-3327-At-1 rat prostate cancer. *Cancer Res.* 1994;54:167–174.

12. Milovanovic SR, Radulovic S, Groot K, Schally AV. Inhibition of growth of PC-82 human prostate cancer cell line xenografts in nude mice by bombesin antagonist RC-3095 or combination of agonist (D-Trp6)-luteinizing hormone-releasing hormone and somatostatin analogue RC-160. *Prostate.* 1992;20:269–280.

13. Jungwirth A, Pinski J, Galvan G, et al. Inhibition of growth of androgen independent DU-145 prostate cancer in vivo by luteinizing hormone-releasing hormone antagonist cetrolix and bombesin antagonists RC-3940-II and RC-3950-II. *Eur J Cancer.* 1997;33:1141–1148.

14. Fathi Z, Way JW, Corjay MH, Viallet J, Sausville EA, Battey JF. Bombesin receptor structure and expression in human lung carcinoma cell lines. *J Cell Biochem Suppl.* 1996;24:237–246.

15. Markwalder R, Reubi JC. Gastrin-releasing peptide receptors in the human prostate: relation to neoplastic transformation. *Cancer Res.* 1999;59:1152–1159.

16. Gugger M, Reubi JC. Gastrin releasing peptide receptors in non-neoplastic and neoplastic human breast. *Am J Pathol.* 1999;155:2067–2076.

17. Corjay MH, Dorasznki DJ, Way JM, et al. Two distint bombesin receptor subtypes are expressed and functional in human lung carcinoma cells. *J Biol Chem.* 1991;266:18771–18779.

18. Nagai MA, Marques LA, Yamamoto L, Fujiyama CT, Brentani MM. Estrogen and progesterone receptor mRNA levels in primary breast cancer: association with patient survival and other clinical and tumor features. *Int J Cancer.* 1994;59:351–356.

19. Maurizi M, Scambia G, Benedetti Panici P, et al. EGF receptor expression in primary laryngeal cancer: correlation with clinico-pathological features and prognostic significance. *Int J Cancer.* 1992;52:862–866.

20. Veale D, Kerr N, Gibson GJ, Kelly PJ, Harris AL. The relationship of quantitative epidermal growth factor receptor expression in non-small cell lung cancer to long term survival. *Br J Cancer.* 1993;68:162–165.

21. Toi-Scott M, Jones CLA, Kane MA. Clinical correlates of bombesin-like peptide receptor subtype expression in human lung cancer cells. *Lung Cancer.* 1996;15:341–354.

22. Saurin JC, Rouault JP, Abello J, Berger F, Remy L, Chayvialle JA. High gastrin releasing peptide receptor mRNA level is related to tumour dedifferentation and lymphatic vessel invasion in human colon cancer. *Eur J Cancer.* 1999;35:125–132.

23. Hofmann TJ, Simpson SD, Smith CJ, et al. Accumulation and retention of ^{99m}Tc RP527 by GRP receptor expressing tumors in SCID mice [abstract]. *J Nucl Med.* 1999;40(suppl):104P.

24. Van de Wiele C, Dumont F, Vanden Broecke R, et al. Tc-99m RP527, a GRP analogue for visualisation of GRP receptor expressing malignancies: a feasibility study. *Eur J Nucl Med.* 2000;11:1649–1699.

25. Hidalgo JU, Nadler SB, Bloch T. The use of electronic digital computer to determine best fit of blood volume formulas [abstract]. *J Nucl Med.* 1962;3(suppl):94P.

26. International Commission on Radiobiological Protection. *Limits for Intakes of Radionuclides by Workers: ICRP Publication 30.* New York, NY: Pergamon Press; 1979.

27. Booij J, Sokole EB, Stabin MG, Janssen AGM, de Bruin K, van Royen EA. Human biodistribution and dosimetry of (^{123}I)FP-CIT: a potent radioligand for imaging of dopamine transporters. *Eur J Nucl Med.* 1998;25:24–30.

28. Loevinger R, Budinger T, Watson E. *MIRD Primer for Absorbed Dose Calculations.* New York, NY: Society of Nuclear Medicine; 1988.

29. Cristy M, Eckerman K. *Specific Absorbed Fractions of Energy at Various Ages from Internal Photon Sources: ORNL/TM 8381/VII.* Oak Ridge, TN: Oak Ridge National Laboratory; 1987:7–29.

30. Stabin MG. MIRDOSE: personal computer software for internal dose assessment in nuclear medicine. *J Nucl Med.* 1996;37:538–546.

31. Bertacinni G, Impicciatore M, Molina E, Zappia L. Action of bombesin on human gastrointestinal motility. *Gastroenterology.* 1974;6:45–51.

32. Bloom SR, Ghatei MA, Christofides ND, et al. Bombesin infusion in man, pharmacokinetics and effect on gastro-intestinal and pancreatic hormonal peptides [abstract]. *J Endocrinol.* 1979;83:51P.

33. Sunday ME, Kaplan LM, Motoyama E, Chin WW, Spindel ER. Gastrin releasing peptide gene expression in health and disease. *Lab Invest.* 1988;59:5–24.

34. Weber CJ, O'Dorisio TM, McDonald TJ, Howe B, Koschitzky T, Merriam L. Gastrin-releasing peptide-, calcitonin gene related peptide- and calcitonin-like immunoreactivity in human breast cyst fluid and gastrin-releasing peptide-like immunoreactivity in human breast carcinoma cell lines. *Surgery.* 1989;106:1134–1140.

35. Halmos G, Wittliff JL, Schally AV. Characterization of bombesin/gastrin releasing peptide receptors in human breast cancer and their relationship to steroid receptor expression. *Cancer Res.* 1995;55:280–287.

36. Levy R, Eustache F, Pilikian S, et al. Effect of gastrin-releasing peptide on sperm functions. *Mol Hum Reprod.* 1996;2:867–872.

37. Hamazaki OH, Wada E, Matsui K, Wada K. Cloning and expression of the neuromedin B receptor and the third subtype of bombesin receptor genes in the mouse. *Brain Res.* 1997;762:165–172.

38. International Commission on Radiological Protection. *Recommendations of the International Commission on Radiological Protection: ICRP Publication 60.* New York, NY: Pergamon Press; 1991.

39. Beekhuis H. Population radiation absorbed dose from nuclear medicine procedures in The Netherlands. *Health Phys.* 1988;54:287–291.

40. World Health Organization. *Technical Report Series 611: Use of Ionizing Radiation and Radionuclides on Human Beings from Medical Research, Training, and Nonmedical Purposes—Report of a World Health Organization Expert Committee.* Geneva, Switzerland: World Health Organization; 1977.